

## Uncertainty Assessment of the Screw Removal System for Robotic Disassembly of Hard Disk Drives During the Recycling Process

R. SZEWCZYK<sup>a,\*</sup>, J. SZAŁATKIEWICZ<sup>b</sup>, M. NOWICKI<sup>a</sup>, P. GAZDA<sup>a</sup>,  
A. OSTASZEWSKA-LIŻEWSKA<sup>a</sup>, P. NOWAK<sup>a</sup>, T. CHARUBIN<sup>a</sup>,  
W. ROGALSKI<sup>b</sup>, M. WIKTOROWICZ<sup>b</sup>, I. PATAPENKA<sup>b</sup>,  
A. SIEMIĄTKOWSKI<sup>c</sup> AND J. ZIELIŃSKI<sup>c</sup>

<sup>a</sup>*Institute of Metrology and Biomedical Engineering, Faculty of Mechatronics, Warsaw University of Technology, św. A. Boboli 8, 02-525 Warsaw, Poland*

<sup>b</sup>*Phoenix-Surowce Ltd., Kasztanowa 18, 05-816 Michałowice-Wieś, Poland*

<sup>c</sup>*Industrial Research Institute for Automation and Measurements PIAP — Łukasiewicz Research Network, Al. Jerozolimskie 202, 02-486 Warsaw, Poland*

Doi: [10.12693/APhysPolA.146.591](https://doi.org/10.12693/APhysPolA.146.591)

\*e-mail: [roman.szewczyk@pw.edu.pl](mailto:roman.szewczyk@pw.edu.pl)

Robotic disassembly of hard disk drives during their recycling process is a promising technology with significant ecological importance and high economic profitability. However, the efficiency of the robotic disassembly of screws in the cost-efficient process using the robotic system in the selective compliance assembly robot arm configuration is highly dependent on the accuracy of positioning. In such a case, the robot works based on known screw positions without a visual control loop. The paper presents the generalised method of analysis of key factors influencing the process, starting from visual geometry analysis to mechanical setup accuracy. The formalised metrological analysis was performed on the base of the Monte-Carlo method to identify the key factors influencing the screw positioning accuracy. It was stated that the robot control uncertainty plays a crucial role in the total uncertainty of the system.

topics: Monte Carlo analysis, uncertainty propagation, uncertainty modelling

### 1. Introduction

Recycling *waste from electrical and electronic equipment* (WEEE) plays a key role in the circular economy [1], reducing the environmental impact [2] of technological development. In addition, such recycling may be the source of valuable raw materials, such as copper [3], aluminium [4], and other metals, including the *critical raw materials* (CRW) rare earth metals [5]. Hard disk drives are among the most interesting subjects in the application of automation in WEEE recycling. It should be highlighted that during the years 2010–2020, over 4 billion *hard disk drives* (HDDs) were produced globally [6]. Over 30% of these devices will be recycled in Europe [7]. It is expected that during the next years, due to conversion from HDDs to *solid state drives* (SSDs) and the wear and tear of the moving parts, over 70 million HDDs will have to be recycled annually.

It should be highlighted that one of the most important problems related to the HDD recycling is connected to the fact that highly sensitive data is stored in recycled HDDs. To achieve a satisfactory level of data safety, EoL (*end of life*) HDDs are mainly shredded [8]. However, this approach significantly reduces the possibility of efficient raw materials recovery.

To avoid these problems, a robotic disassembly process was proposed. In this process, the disk data-storing plates are separated and melted, whereas other elements are disassembled and recycled separately. As a result, the robotic disassembly of HDDs guarantees a high data safety level and enables efficient raw materials recovery. This is especially important considering the neodymium hard magnets, which can be easily separated during disassembly instead of being lost during shredding.

On the other hand, to achieve high speed and economic efficiency of the HDD robotic disassembly, the process has to be performed without a direct

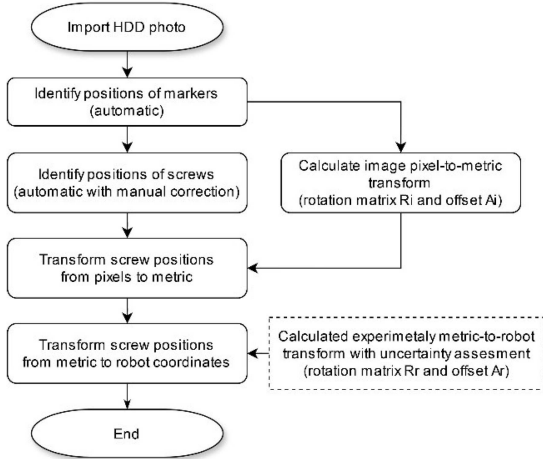


Fig. 1. Schematic block diagram of screw removal during robotic disassembly of hard disk drives in the recycling process.

visual control loop between the robot and the processed HDD. As a result, the accuracy of robotised screwdriver positioning against the heads of the screws plays a key role in the reliability of the disassembly process. To achieve such a high level of reliability, the accurate and easy-for-application model of uncertainty propagation in the disassembly systems should be elaborated. It should be highlighted that it is difficult to apply the commonly used differential models of uncertainty propagation [9] due to the high non-linearity and sophistication of uncertainty transmission.

The paper presents a Monte Carlo approach-based model of uncertainty propagation in the robotic disassembly process. The presented model enables testing the significance of all sources of uncertainty from the visual analyses up to the positioning of the screwdriver robotic head working in the *selective compliance assembly robot arm* (SCARA). In addition, the proposed approach may be easily generalised to other types of robotised systems requiring precise positioning.

## 2. The structure of the system

The schematic block diagram of the robotic arm control idea is presented in Fig. 1, whereas the photograph presenting the implementation of the system is presented in Fig. 2.

In the first step, the photograph of HDD is taken. An example of such photograph is presented in Fig. 3. During the photographing, HDD is located in a special mechanical measuring slot (element 1 in Fig. 2 and element 2 in Fig. 3). Next, the positioning markers (elements 3 in Fig. 3) are identified during the automated visual analyses utilising Hough's transform [10]. Since the positions of markers are

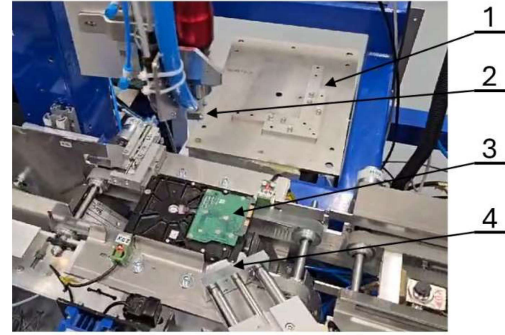


Fig. 2. General view of robotic disassembly station: 1 — geometry measurement sub-system, 2 — SCARA robot with the screwdriver, 3 — disassembled HDD, 4 — mechanical slot.



Fig. 3. Geometry measurement sub-system: 1 — disassembled HDD, 2 — measuring slot, 3 — markers, 4 — screws.

known in advance (based on accurate measurements), the first image pixel-to-metric transform can be calculated. This transform consists of a  $3 \times 3$  rotation matrix  $R$  and a  $3 \times 1$  offset vector  $A$ .

Next, the screw positions are identified utilising Hough's transform together with a convolutional neural network classifier [11]. An example of the identified screw is presented as element 4 in Fig. 3. It should be highlighted that the screw identification process is semi-automatic and always verified by the operator.

Finally, the metric position of the screws in a photograph has to be transformed into a SCARA robot coordinating system. This process requires another set of  $3 \times 3$  rotation matrix  $R_t$  and  $3 \times 1$  offset vector  $A_t$ .

To determine the matrix  $R_t$  and vector  $A_t$ , measurements of screwdriver head positioning were carried out on the well-described HDDs examples. However, due to practical reasons, the head of the screwdriver exhibits significant clearance, enabling efficient screwing and unscrewing. These clearances are the most important reasons for the uncertainty assigned to values in the matrix  $R_t$  and vector  $A_t$ .

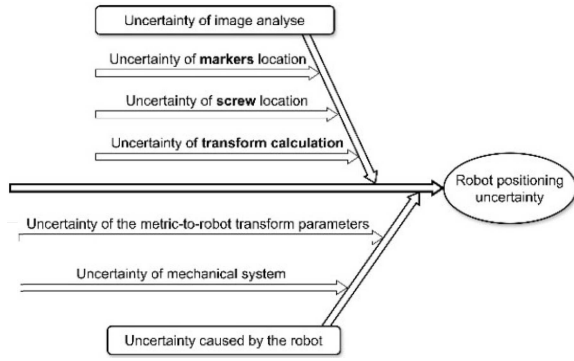


Fig. 4. Ishikawa diagram (fishbone diagram) of uncertainty propagation in the process.

TABLE I

Sources of uncertainty in image processing during the screw removal process.

Source	Distribution	Parameter	Value
markers location	normal*	standard deviation	4 pixels
screw location	normal*	standard deviation	8 pixels
pixel-to-metric transform	neglected	–	–

\*limited to 3 standard deviations

Finally, during the SCARA robot operation, the criterion for a successful unscrew process is connected with the location of the screwdriver head at a distance less than 1.7 mm from the centre of the screw's head. In such a case, an automatic screwdriver head can find the screw slot during the spiral rotation process. If the distance exceeds 1.7 mm from the centre of the screw's head, the screwdriver will fall out from the screw head and miss the slot causing unsuccessful unscrewing.

### 3. Main sources of uncertainty

The Ishikawa diagram (fishbone diagram) of uncertainty propagation in screw removal during the process of the robotic disassembly of the hard disk drives is presented in Fig. 4. The two main sources of uncertainty are connected with the image analyses and the SCARA robotic arm operation.

Quantitative analyses of the sources of uncertainty in image processing are summarised in Table I. It should be highlighted that typically the influencing factors exhibit a distribution close to normal. However, uncertainty values higher than three standard deviations were removed due to the fact that such values do not occur in the real system.

TABLE II

Estimators of the standard deviation of the parameters in the matrix  $R_t$  and vector  $A_t$  determined experimentally.

Parameter	Value	The estimator of standard deviation
$R_t(1, 1)$	-0.015	0.009
$R_t(1, 2)$	0.985	0.005
$R_t(2, 1)$	-0.985	0.006
$R_t(2, 2)$	-0.013	0.008
$A_t(1, 1)$	156.1	1.2
$A_t(2, 1)$	11.3	1.4

Estimators of standard deviations describing the uncertainties assigned to the values in the matrix  $R_t$  and vector  $A_t$  were determined experimentally by 7 repetitions and presented in Table II. In this case, the extension coefficient according to the t-Student distribution was used.

### 4. Monte Carlo uncertainty propagation model

The Monte Carlo simulation was carried out to model the propagation of uncertainty. The model was implemented in Octave — an open-source alternative of MATLAB software. The screw removal process presented in Fig. 1 was simulated  $10^6$  times, and the uncertainty of the results of modelling was observed.

During the simulation, the position of the modelled screw was determined with uniform distribution in the range where the screw is expected in the photograph. Parameters influenced by uncertainty were modelled according to the distributions and parameters presented in Tables I and II.

The results of Monte Carlo modelling are presented in Fig. 5. The uncertainty of screw location in both the  $x$  and  $y$  axes is described by the normal distribution (Fig. 5a and b) with standard deviation estimators equal to 1.04 and 1.09 mm, respectively. The difference in values of standard deviation is caused by the fact that the area of possible screw location is rectangular (as presented in Fig.3).

The distribution of the distance from the real screw centre location is presented in Fig. 5c. Since the normal distribution describes the uncertainties of both the  $x$  and  $y$  axes, the distribution of distances follows the Rayleigh distribution.

Considering the success criteria presented previously, 72.3% of the tries fit in the distance lower than 1.7 mm from the screw centre. This result aligns with practical tests performed at the robotic disassembly station presented in Fig. 2.

### 5. Main sources of uncertainty and sensitivity analysis

The presented Monte Carlo method of uncertainty modelling enables the analysis of both the participation of a given uncertainty source in the total uncertainty of the process, as well as the total uncertainty sensitivity on a selected parameter. In this case, the total uncertainty sensitivity  $\gamma$  can be defined as

$$\gamma = \frac{\Delta s_T}{\Delta s_i}, \quad (1)$$

where  $\Delta s_T$  is the relative change in the total uncertainty and  $\Delta s_i$  is the relative 10% change in the uncertainty of a given parameter  $i$ . The participation of the analysed uncertainty sources in the total uncertainty of the process, together with the total uncertainty sensitivities, are presented in Table III.

TABLE III

Reduction of total uncertainty of the process without the uncertainty source and the total uncertainty sensitivities (from the point of view of standard deviation estimators of  $dx$  and  $dy$ , respectively).

Parameter	Reduction of total uncertainty without the uncertainty source	Total uncertainty sensitivity
markers location	negligible	N/A
screw location	3%/3%	negligible
pixel-to-metric transf.	negligible	N/A
$R_t(1,1)$	15%/0%	0.2/0.0
$R_t(1,2)$	2.5%/0%	0.1/0.0
$R_t(2,1)$	0%/6.2%	0.0/0.15
$R_t(2,2)$	0%/6.3%	0.0/0.12
$R_t$	18%/12%	0.3/0.2
$A_t(1,1)$	32%/0%	0.5/0.0
$A_t(2,1)$	0%/43%	0.0/0.6
$A_t$	33%/43%	0.5/0.7

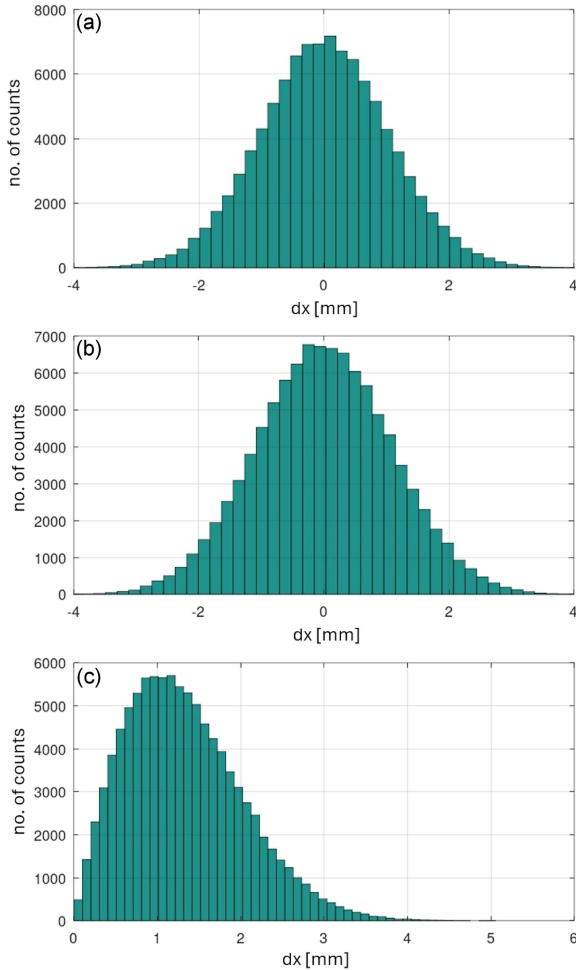


Fig. 5. Results of Monte-Carlo simulation of robot positioning uncertainty: (a) uncertainty in  $x$  direction (normal distribution), (b) uncertainty in  $y$  direction (normal distribution), (c) uncertainty of positioning distance from the screw centre (Rayleigh distribution).

The presented results clearly indicate that the accuracy of determining the values in the matrix  $R_t$  and vector  $A_t$  plays a key role in the total uncertainty of the modelled system. As a result, to increase the success ratio connected with a less than 1.7 mm error of the screw centre positioning, the accuracy of experimental determination of the matrix  $R_t$  and vector  $A_t$  has to be improved. From a practical point of view, this can only be achieved by developing a special mechanical setup that stabilises the working point of the screwdriver and reduces its clearances.

### 6. Conclusions

The Monte Carlo simulation-based method presented in the paper enables efficient and accurate modelling of uncertainty propagation in sophisticated systems, where differential analyses are sophisticated or impossible due to the high nonlinearity of the transfer function. Moreover, the presented method may implement experimentally determined the statistical uncertainty distributions. As a result, e.g., the uncertainty of a given parameter can be limited to a value less than three times the standard deviation value.

The proposed method enables not only the calculation of the total value of uncertainty but also gives the unique possibility of direct estimation of the participation of the uncertainty source in the total uncertainty of the process, as well as the total uncertainty sensitivities. In the presented case, it was determined that the accuracy of the determining the values in the matrix  $R_t$  and vector  $A_t$  (connected with the positioning of the robotic arm of the SCARA robot) plays a key role in the total uncer-

tainty of the modelled system. This finding creates the possibility for a clearly targeted further development of the hard disk drive's robotic disassembly process to increase its efficiency and accuracy.

### Acknowledgments

The research was carried out within EUREKA project no EUREKA/AI-REC/13/2022 project co-financed by the National Centre for Research and Development (NCBR) in the years 2024–2025.

### References

- [1] Y. van Fan, J.J. Klemes, C.T. Lee, in: *2021 6th Int. Conf. on Smart and Sustainable Technologies (SpliTech)*, IEEE, 2021, p. 1.
- [2] K. Hassan, P. Kaur, V. Vijayasingam, in: *2023 Int. Conf. on Integrated Intelligence and Communication Systems (ICI-ICS)*, IEEE, 2023, p. 1.
- [3] R. Suryawanshi, K. Chatrapathy, A. Al-Khaykan, W.D. Priya, Ch.V. Reddy, K.V.S. Prasad, in: *2023 7th Int. Conf. on Image Information Processing (ICIIP)*, IEEE, 2023, p. 411.
- [4] M. Aboughaly, H.A. Gabbar, in: *E-waste Recycling and Management*, Springer, Cham 2019, p. 63.
- [5] R.H. Koppelaar, S. Pamidi, E. Hajósi et al., *Sustainability* **15**, 1405 (2023).
- [6] T. Alsop, *Hard disk drive (HDD) unit shipments worldwide from 1976 to 2022*, Statista 2023.
- [7] Maximize Market Research, *SAS Hard Disk Drives Market — Global Industry Analysis and Forecast (2024-2030) — by Type, Storage Capacity, Industry and Region*, 2023.
- [8] M. Mutemwa, F. Mouton, in: *2018 Conf. on Information Communications Technology and Society (ICTAS)*, IEEE, 2018, p. 1.
- [9] D. Barchiesi, T. Grosgees, *J. Opt. Soc. Am. A* **34**, 1602 (2017).
- [10] X. Zhou, Y. Ito, K. Nakano, in: *2014 2nd Int. Symp. on Computing and Networking*, IEEE, 2024 p. 447.
- [11] Y. Shen, X. Hu, T. Wang, J. Cui, S. Tao, A. Li, Q. Lu, D. Zhang, W. Xiao, *Appl. Geophys.* **20**, 252 (2023).